

# Logarithmic scaling in the near-dissipation range of turbulence

K.R. Sreenivasan<sup>1</sup>, A. Bershadskii<sup>1,2</sup>

<sup>1</sup>The Abdus Salam International Center for Theoretical Physics, Strada Costiera 11, 34100 Trieste, Italy

<sup>2</sup>ICAR, P.O. Box 31155, Jerusalem 91000, Israel

A logarithmic scaling for structure functions, in the form  $S_p \sim [\ln(r/\eta)]^{\zeta_p}$ , where  $\eta$  is the Kolmogorov dissipation scale and  $\zeta_p$  are the scaling exponents, is suggested for the statistical description of the near-dissipation range for which classical power-law scaling does not apply. From experimental data at moderate Reynolds numbers, it is shown that the logarithmic scaling, deduced from general considerations for the near-dissipation range, covers almost the entire range of scales (about two decades) of structure functions, for both velocity and passive scalar fields. This new scaling requires two empirical constants, just as the classical scaling does, and can be considered the basis for extended self-similarity.

PACS numbers: 47.27.-i, 47.27.Gs, 47.27.Nz

The Kolmogorov approach to the phenomenological description of the inertial range of scales in turbulence requires that the scales  $r \gg \eta$ , where  $\eta$  is Kolmogorov dissipation scale [1]. The dominant physical mechanism operating in the inertial range can be thought to be the Kolmogorov-Richardson cascade, and its application readily yields the well-known power-law scaling [2, 3]. On the other hand, the near-dissipation range of scales, for which  $r > \eta$  but there exists no separation between the inertial and dissipation ranges, has a more complex dynamics arising from a strong competition between the cascade and dissipation mechanisms (see, for instance, Refs. [4],[5],[6] and the references cited there). Indeed, for small and moderate Reynolds numbers, the near-dissipation range can span most of the available range of scales. Analogous situation occurs also for the turbulent mixing of passive scalars.

One of the few properties known about the near-dissipation region is that it obeys the so-called Extended Self-Similarity (ESS) [7], while the classical power-law

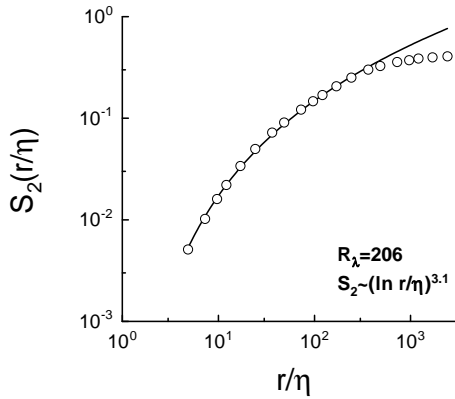


FIG. 1: The second order structure function  $S_2(r/\eta)$  against  $r/\eta$ . The experimental data ( $R_\lambda = 206$ ) are shown as circles. The solid curve is the best fit of (3) to the data, corresponding to the logarithmic scaling.

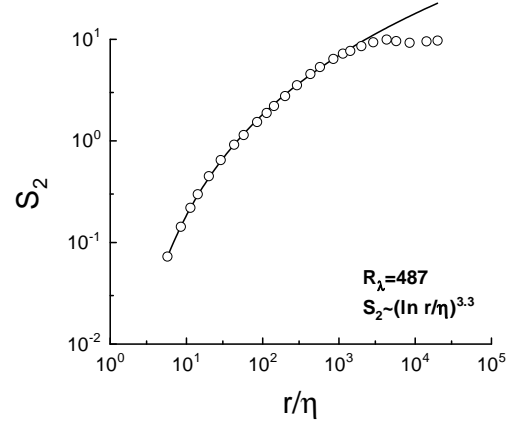


FIG. 2: The same as in Fig. 1 but for  $R_\lambda = 487$ .

scaling does not exist. In ESS the scaling relation between structure functions of different orders is given by

$$S_p(r) \sim S_q^{\beta_{p,q}}(r), \quad (1)$$

where  $\beta_{p,q}$  is the exponent of the  $p$ -th order structure function relative to that of the  $q$ -th order. For the velocity field in the near-dissipation range, ESS implies that

$$S_p(r) = f(r/\eta)^{\zeta_p}, \quad (2)$$

where  $f(x)$  is an unknown function different from a power law. Finding this function is crucial for the near-dissipation range. We show here, using experimental and numerical data, that the logarithmic function

$$S_p \sim [\ln(r/\eta)]^{\zeta_p} \quad (3)$$

can successfully replace the power law  $S_p \sim r^{\zeta_p}$  in the near-dissipation range.

Figures 1 and 2 show the longitudinal second order structure function of the velocity field calculated using the data obtained in a wind tunnel at  $R_\lambda = 206$  and 487, respectively. Here  $R_\lambda$  is the so-called Taylor microscale Reynolds number which varies as the square root of the

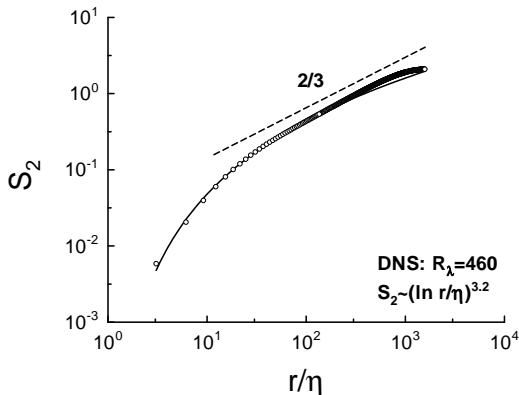


FIG. 3: The second order structure function  $S_2(r/\eta)$  against  $r/\eta$ . The DNS data [9] ( $R_\lambda = 460$ ) are shown as circles. The solid curve is the best fit of (3) corresponding to the logarithmic scaling. The dashed straight line is the Kolmogorov's 2/3-rds scaling form, nominally thought to be applicable in the inertial range (ignoring effects of small-scale intermittency).

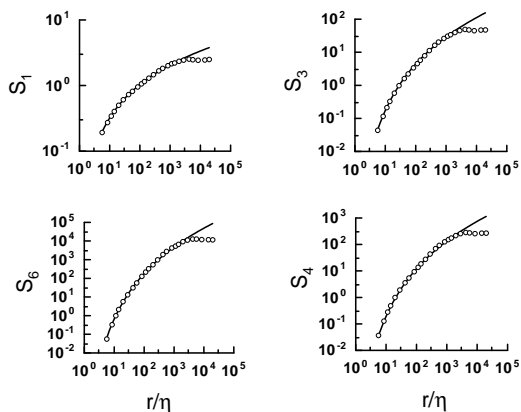


FIG. 4: Structure functions of different orders ( $p = 1, 3, 4$  and  $6$ ) for  $R_\lambda = 487$  (cf. Fig. 2). The solid curves are drawn to indicate the logarithmic scaling (3).

large-scale Reynolds number. The flow was a combination of the wake and homogeneous turbulence behind a grid and is fully described in Ref. [8]. Following convention, we invoke Taylor's hypothesis [1] to equate temporal statistics to spatial statistics. We normalize the scale  $r$  by the Kolmogorov scale  $\eta$ . The solid curves in these figures are the best fit by equation (3) for  $\zeta_2 \simeq 3.1$  and  $3.3$ , respectively. For comparison, we show in Fig. 3 the quantity  $S_2(r)$  calculated using data from a high-resolution direct numerical simulation of homogeneous steady three-dimensional turbulence [9], corresponding to  $1024^3$  grid points and  $R_\lambda = 460$ . The solid curve in this figure also corresponds to the best fit by equa-

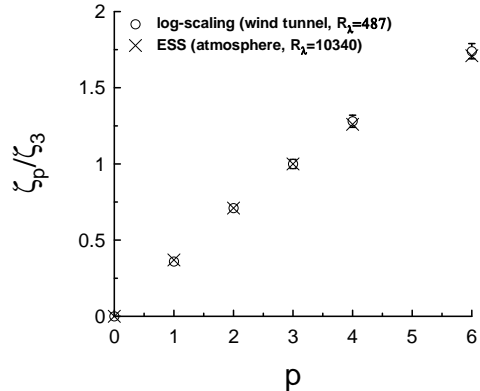


FIG. 5: Normalized exponents  $\zeta_p/\zeta_3$  against  $p$  for  $R_\lambda = 487$  (circles). Crosses are the ESS exponents obtained for the atmospheric turbulence data at  $R_\lambda = 10340$  [10].

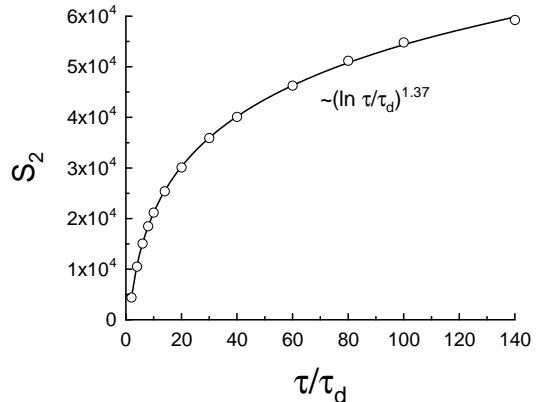


FIG. 6: Second order structure function of the temperature fluctuations for the heated wake.

tion (3), with  $\zeta_2 \simeq 3.2$ . The logarithmic scaling applies well to the near-dissipation region and, although we don't particularly expect it, to a considerable part of the inertial range as well, overlapping with the 2/3-rds form of Kolmogorov.

Figure 4 shows the structure functions of different orders for wind-tunnel data ( $R_\lambda = 487$ ) and the logarithmic scaling (3) is shown in the figure as the solid curves. The exponents  $\zeta_p$  normalized by the exponent  $\zeta_3$  are shown in Fig. 5 as circles. For comparison we show by crosses in this figure the normalized exponents obtained using ESS in the atmospheric turbulence for large  $R_\lambda = 10340$  [10]. As described at some length in [10], the ESS exponents are very close to those determined directly.

The fact that the logarithmic exponents are also the same as the power law exponents clearly shows why the

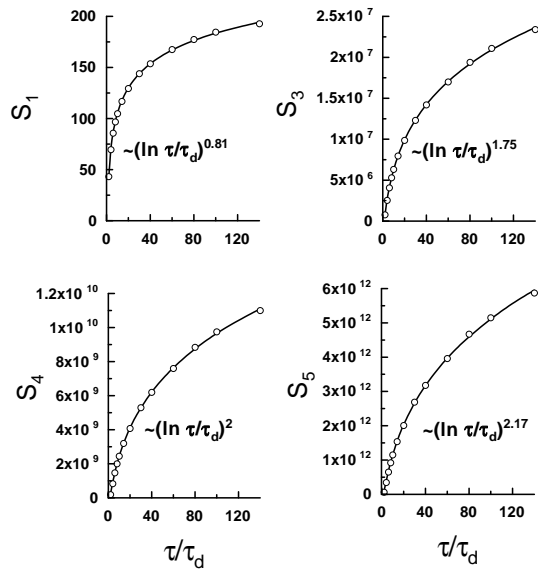


FIG. 7: As in Fig. 3 but for different orders of the structure function.

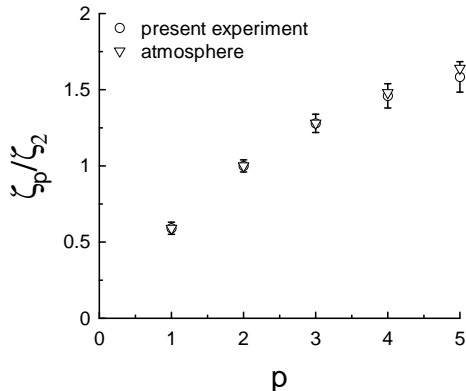


FIG. 8: Exponents for the passive scalar extracted from Figs. 6 and 7 (circles) and for the fully developed atmospheric turbulence (ordinary scaling in the inertial interval, triangles [12]).

ESS works well at low Reynolds numbers. We understand that this observation merely shifts emphasis on explaining why these two sets of exponents should be identical, but leave this question for the future.

For the passive scalar we use the data acquired with a cold-wire probe in the wake of a heated cylinder in a wind tunnel (see Ref. [11] for details of the experiment). Temperature can be considered a passive scalar for the conditions of the experiment. We used measurements on the centerline of the wake. Figures 6 and 7 show

the temperature structure functions of different orders and the solid curves are the best fits drawn to indicate agreement with equation (3) (i.e., logarithmic scaling). Values of  $\zeta_p/\zeta_2$  calculated from Figs. 6 and 7 are shown

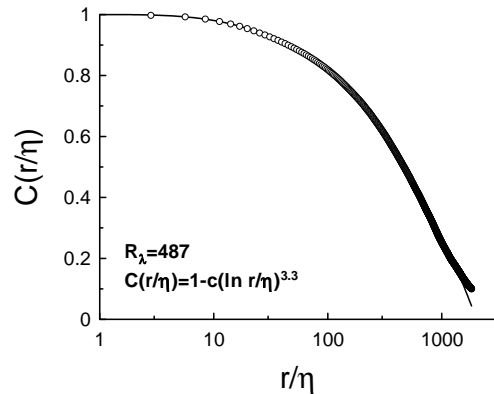


FIG. 9: Correlation function for velocity fluctuations against  $r/\eta$  for  $R_\lambda = 487$  (circles). The solid curve is drawn in the figure to indicate agreement with the logarithmic scaling shown in Fig. 2.

in Fig. 8 as circles. We also show by triangles in this figure the ESS exponents obtained for passive scalar in fully developed atmospheric turbulence using *ordinary* scaling in the *inertial* range of scales [12].

It should be pointed out that the logarithmic scaling requires two fitting constants just as the ordinary scaling does, and, in the examples discussed above, the range of scales covered by this scaling is about two decades. Application of these results to correlation functions and spectra is in good agreement with the structure functions analysis (see, for instance, Fig. 9) as well as with other available data sets.

Thus, we have clear experimental indication that the logarithmic scaling is an appropriate tool for the description of data in the near-dissipation range. This scaling applies to nearly the entire range of scales in flows of low and modest Reynolds numbers. At high Reynolds numbers, it overlaps with the conventional power laws. The logarithmic exponents are the same as the classical ones, thus demonstrating why ESS works so well at low and moderate Reynolds numbers. These comments apply to both velocity and scalar fields. The theory concerning these observations will be discussed elsewhere [13].

We thank Bruce Pearson and Toshi Gotoh for sharing their data.

[1] A.S. Monin and A.M. Yaglom, *Statistical Fluid Mechanics*, Vol. 2, (MIT Press, Cambridge 1975)

[2] U. Frisch, *Turbulence* (Cambridge University Press, Eng-

- land, 1995)
- [3] K.R. Sreenivasan and R.A. Antonia, *Annu. Rev. Fluid Mech.* **29**, 435 (1997)
  - [4] M. Nelkin, *Adv. Phys.* **43**, 143 (1994).
  - [5] C. Meneveau, *Phys. Rev. E* **54**, 3657 (1996)
  - [6] L. Chevillard, B. Castaing, E. Leveque, On the Rapid Increase of Intermittency in the Near-Dissipation Range of Fully Developed Turbulence, *cond-mat/0311409* (2003)
  - [7] R. Benzi, L. Biferale, S. Ciliberto, M.V. Struglia and R. Tripiccion, *Physica D* **96**, 162 (1996)
  - [8] B.R. Pearson, P.-A. Krogstad and W. van de Water, *Phys. Fluids* **14**, 1288 (2002)
  - [9] T. Gotoh, D. Fukayama and T. Nakano, *Phys. Fluids*, **14**, 1065 (2002)
  - [10] K.R. Sreenivasan and B. Dhruva, *Prog. Theor. Phys. Suppl.* **130**, 103 (1998)
  - [11] P. Kailasnath, K.R. Sreenivasan and J.R. Saylor, *Phys. Fluids A* **5**, 3207 (1993)
  - [12] F. Schmidt, D. Schertzer, S. Lovejoy and Y. Brunet, *Europhys. Lett.* **34**, 195 (1996)
  - [13] A. Bershadskii and K.R. Sreenivasan, in preparation